



Contents lists available at ScienceDirect

Biochemical and Biophysical Research Communications

journal homepage: [www.elsevier.com/locate/ybbrc](http://www.elsevier.com/locate/ybbrc)



# PPAR $\gamma$ and MyoD are differentially regulated by myostatin in adipose-derived stem cells and muscle satellite cells



Feng Zhang<sup>a</sup>, Bing Deng<sup>b</sup>, Jianghui Wen<sup>c</sup>, Kun Chen<sup>a</sup>, Wu Liu<sup>b</sup>, Shengqiang Ye<sup>b</sup>, Haijun Huang<sup>b</sup>, Siwen Jiang<sup>a,\*</sup>, Yuanzhu Xiong<sup>a,\*</sup>

<sup>a</sup> Key Laboratory of Swine Genetics and Breeding of the Agricultural Ministry and Key Laboratory of Agricultural Animal Genetics, Breeding and Reproduction of the Ministry of Education, College of Animal Science and Technology, Huazhong Agricultural University, Wuhan, 430070, PR China

<sup>b</sup> Wuhan Institute of Animal Science and Veterinary Medicine, Wuhan Academy of Agricultural Science and Technology, Wuhan, Hubei, 430208, PR China

<sup>c</sup> Wu Han University of Technology, Wuhan 430074, PR China

## ARTICLE INFO

### Article history:

Received 17 January 2015

Available online 31 January 2015

### Keywords:

Myostatin

Adipose-derived stem cells

Muscle satellite cells

PPAR $\gamma$

MyoD

## ABSTRACT

Myostatin (MSTN) is a secreted protein belonging to the transforming growth factor- $\beta$  (TGF- $\beta$ ) family that is primarily expressed in skeletal muscle and also functions in adipocyte maturation. Studies have shown that MSTN can inhibit adipogenesis in muscle satellite cells (MSCs) but not in adipose-derived stem cells (ADSCs). However, the mechanism by which MSTN differentially regulates adipogenesis in these two cell types remains unknown. Peroxisome proliferator-activated receptor- $\gamma$  (PPAR $\gamma$ ) and myogenic differentiation factor (MyoD) are two key transcription factors in fat and muscle cell development that influence adipogenesis. To investigate whether MSTN differentially regulates PPAR $\gamma$  and MyoD, we analyzed PPAR $\gamma$  and MyoD expression by assessing mRNA, protein and methylation levels in ADSCs and MSCs after treatment with 100 ng/mL MSTN for 0, 24, and 48 h. PPAR $\gamma$  mRNA levels were downregulated after 24 h and upregulated after 48 h of treatment in ADSCs, whereas in MSCs, PPAR $\gamma$  levels were downregulated at both time points. MyoD expression was significantly increased in ADSCs and decreased in MSCs. PPAR $\gamma$  and MyoD protein levels were upregulated in ADSCs and downregulated in MSCs. The CpG methylation levels of the PPAR $\gamma$  and MyoD promoters were decreased in ADSCs and increased in MSCs. Therefore, this study demonstrated that the different regulatory adipogenic roles of MSTN in ADSCs and MSCs act by differentially regulating PPAR $\gamma$  and MyoD expression.

© 2015 Elsevier Inc. All rights reserved.

## 1. Introduction

Intramuscular fat is indicated by the appearance of white flecks or streaks of adipose tissue between bundles of muscle fibers in skeletal muscle [1]. The presence of intramuscular fat is one of the main factors used to determine meat quality grades and plays an important role in the animal production industry [2]. Adipocytes in muscles are of great concern because these cells are associated with the meat quality in animal production [2,3] and they are also associated with insulin resistance in humans [4,5]. However, the origin of adipocytes in muscle tissue remains unclear. Pethick et al. [6] hypothesized that adipocytes in muscle tissue can be differentiated from stem cells in the muscle, including adipose-derived

stem cells (ADSCs) and muscle satellite cells (MSCs). This hypothesis has been partially confirmed in vitro [3,7,8]. Deng et al. [9] discovered that myostatin (MSTN), a member of the transforming growth factor- $\beta$  (TGF- $\beta$ ) superfamily, inhibits the adipogenic potential of MSCs but not ADSCs at the stage of commitment. From these results, the authors hypothesized that adipocytes in muscle may originate from ADSCs, but their studies did not elucidate the mechanism by which MSTN differentially regulates ADSC and MSC adipogenesis.

Numerous studies have demonstrated that MSTN exhibits different adipogenic functions in different stem cells. For example, Artaza et al. [10] demonstrated that MSTN promotes the differentiation of multipotent mesenchymal cells into preadipocytes, whereas Kim et al. [11] showed that MSTN inhibits preadipocyte differentiation. These results indicated that the role of MSTN in adipogenesis could differ depending on the different stages of commitment and differentiation.

\* Corresponding authors. Fax: +86 27 87280408.

E-mail addresses: [jiangsiwen@mail.hzau.edu.cn](mailto:jiangsiwen@mail.hzau.edu.cn) (S. Jiang), [xiongyzhu@163.com](mailto:xiongyzhu@163.com) (Y. Xiong).

Peroxisome proliferator-activated receptor- $\gamma$  (PPAR $\gamma$ ) is a critical transcription factor in adipocyte terminal differentiation. To our knowledge, adipogenesis is not triggered in the absence of PPAR $\gamma$  [11–13]. Myogenic differentiation factor (MyoD) is a transcription factor involved in the regulation of muscle development [10]. The ectopic expression of *MyoD* inhibits adipogenesis in adipose tissue and results in the production of myocytes [14]. PPAR $\gamma$  and MyoD are two key transcription factors in fat and muscle cell development that influence adipogenesis and can be regulated by MSTN. For example, Kim et al. [11] reported that MSTN inhibits 3T3-L1 preadipocyte differentiation through PPAR $\gamma$ . MSTN can also regulate the balance between the proliferation and differentiation of embryonic muscle progenitors by activating *MyoD* [15]. Deng et al. [9] reported that at the commitment stage, MSTN differentially regulated adipogenesis in ADSCs and MSCs. However, it remains unclear whether the key transcription factors PPAR $\gamma$  and MyoD are regulated by MSTN to generate the differences adipogenesis in ADSCs and MSCs.

Thus, in this study, we analyzed PPAR $\gamma$  and MyoD mRNA, protein and methylation levels in the two types of cells. These results will help us understand how MSTN can differentially regulate adipogenesis in ADSCs and MSCs and will also help to elucidate the origin of adipocytes in muscle tissue.

## 2. Materials and methods

### 2.1. Isolation of porcine ADSCs and MSCs

Large white pigs (2–4 days old) were provided by the Jingpin Pig Station of Huazhong Agricultural University and were euthanized by a lethal injection of sodium pentobarbital. Porcine ADSCs were isolated from the subcutaneous fat following a previously described method with minor modifications [9,16]. In brief, fat tissue was excised and finely chopped into 1-mm<sup>3</sup> pieces with scissors in phosphate-buffered saline (PBS) and then incubated for 90 min at 37 °C in 0.1% collagenase type I (Sigma). After enzymatic digestion, the released fat stromal cells were suspended in Dulbecco's Modified Eagle's Medium (DMEM; Gibco) supplemented with 15% fetal bovine serum (FBS; Gibco), and the suspension was filtered through a 40- $\mu$ m nylon mesh. Then, the cells were collected by centrifugation at 2000 rpm for 5 min. The cells were added to fresh DMEM supplemented with 15% FBS and 100 U/mL penicillin/streptomycin. The cells were then plated in Nunclon flasks and cultured in an atmosphere of 5% CO<sub>2</sub> at 37 °C. After 12 h, the non-adherent cells were removed. When the ADSCs achieved 80–90% confluence, they were passaged by trypsinization.

MSCs were isolated from the semitendinosus muscle of the same pig used to isolate ADSCs following a modification of the method described by Yamanouchi et al. [17]. In brief, muscle tissue was excised from the semitendinosus muscle of the hind leg and minced into 1-mm<sup>3</sup> pieces with scissors in PBS after the visible fat and connective tissue were removed. The muscle tissue sample was digested at 37 °C in 0.8% pronase (Sigma) for 50 min. The released cells were suspended in DMEM supplemented with 15% FBS and filtered through a 40- $\mu$ m nylon mesh. The cells were then collected and cultured using the same protocol described for the ADSCs.

### 2.2. Immunohistochemistry

Porcine ADSCs and MSCs were seeded onto sterile clean slides and cultured for 24 h. The cells were then fixed in 4% paraformaldehyde at room temperature for 15 min. After fixation, the cells were washed with PBS, blocked with FBS and incubated with

biotinylated rat anti-mouse antibodies against desmin (Boster; China) and CD44 (Boster; China), following the methods described by Artaza et al. [10].

### 2.3. ADSC and MSC adipogenesis and Oil Red O staining

ADSCs and MSCs were seeded in 6-well plates until confluent. After reaching confluence, the cells were treated with DIM (1  $\mu$ mol/L dexamethasone [Dex] + 1  $\mu$ g/mL insulin + 0.5 mmol/L isobutyl-1-methylxanthine [IBMX]; each from Sigma) for 2 days (from day 0 to day 2). Then, the medium was replaced with DMEM containing 1  $\mu$ g/mL insulin for an additional 2 days (from day 2 to day 4). Last, the medium was replaced with DMEM containing 10% FBS (from day 4 to day 8). Cells cultured with DMEM containing 10% FBS served as controls.

ADSCs and MSCs were washed with PBS, fixed in 4% paraformaldehyde for 15 min, and washed again with PBS. The cells were then stained via incubation with Oil Red O (0.5 g of Oil Red O; Sigma) in 100 mL of isopropanol diluted with water (60:40) for 1 h. After staining, the slides were washed twice in water and then photographed.

### 2.4. DNA/RNA isolation

The ADSCs and MSCs were seeded in 6-well plates until they reached confluence. Then, the cells were collected to extract the DNA and RNA after treatment with 100 ng/mL MSTN for 0, 24, and 48 h. The genomic DNA and total RNA were isolated using All-In-One DNA/RNA Mini-Preps Kit (Sangon; China) according to the manufacturer's protocol.

### 2.5. Quantitative real-time polymerase chain reaction (qPCR) analysis

To quantify the mRNA levels, cDNA was synthesized using a RevertAid First Strand cDNA Synthesis Kit (Thermo Scientific) following the manufacturer's protocol. qPCR was performed in triplicate using the iQ SYBR green Supermix (Bio-Rad) on a LightCycler<sup>®</sup> 480 (Roche). The mRNA level was normalized to  $\beta$ -actin as a house-keeping gene. The primer sequences used for the amplification of  $\beta$ -actin, PPAR $\gamma$  and MyoD are listed in Table 1. The relative mRNA expression levels of the target genes were calculated as the fold changes of the threshold cycle (Ct) value relative to the reference using the  $2^{-\Delta\Delta Ct}$  method. The Ct values of all of the samples were calculated from the mean Ct of triplicate reactions using the following equation:  $\Delta Ct = Ct(\text{target gene}) - Ct(\text{reference gene})$ . Then, the samples were normalized to the calibrator using the following equation:  $\Delta\Delta Ct = \Delta Ct(\text{target gene}) - \Delta Ct(\text{calibrator})$ . The calibrator was an untreated control or cells at a particular stage of development based on comparative results [18]. In this study, the 0 h time point was chosen as the calibrator sample to evaluate the putative differential mRNA expression of the target genes.

### 2.6. DNA bisulfite modification, PCR amplification and sequencing

Genomic DNA was bisulfite-modified using the EpiTect Bisulfite Kit (QIAGEN) according to the manufacturer's protocol. Bisulfite treatment to convert all of the cytosine residues except for 5-methylcytosine to uracil was performed using established protocols. Bisulfite PCR amplification (bPCR) was performed using Ex Taq<sup>®</sup> Hot Start Version (TaKaRa), and the primer sequences used to amplify PPAR $\gamma$  and MyoD are listed in Table 1. The PCR products were recovered using a Gel Extraction Kit (OMEGA) after electrophoresis in 1.5% agarose, and the purified PCR products were cloned

**Table 1**  
Primers used in this study.

Primer Name	Forward 5'–3'	Reverse 5'–3'	Tm °C	Amplicon (bp)
qPCR- $\beta$ -actin	CCAGGTCATCACCATCGG	CCGTGTTGGCGTAGAGGT	58	158
qPCR-PPAR $\gamma$	GCTGACCAAGCAAAGGC	ACGGAGCGAACTGACACC	55	189
qPCR-MyoD	AAGTCAACGAGGCCTTCGAG	GGGGGCCGCTATAATCCATC	58	279
bPCR-PPAR $\gamma$	ATTGGAGTTGTAGTTATTGTTTAT	TAACAAATCTAACTAAATACCATAA	52	162
bPCR-MyoD	GTTGTTATGTGTGTTTTTTTATTA	ACAAAACCTAACACCCAAACAATT	51	224

Abbreviations: qPCR, quantitative real-time PCR; bPCR, bisulfite PCR; bp, base pairs; Tm, melting temperature.

into the pMD18-T vector (TaKaRa). At least 10 insert-positive plasmid clones were sequenced by Sangon Biotech (Shanghai, China).

### 2.7. Western blot analyses of MyoD, PPAR $\gamma$ and $\beta$ -actin

Cells were grown in 6-well plates and treated with 100 ng/mL MSTN for 0, 24, and 48 h. The cells were then collected to measure the levels of PPAR $\gamma$ , MyoD and  $\beta$ -actin (Santa Cruz) by Western blot according to the methods of Kim et al. [11].

### 2.8. Bioinformatics

The PPAR $\gamma$  and MyoD promoter sequences were obtained from the National Center for Biotechnology Information (NCBI; <http://www.ncbi.nlm.nih.gov>). CpG islands were predicted by MethPrimer (<http://www.urogene.org/cgi-bin/methprimer/methprimer.cgi>). QUMA was used to analyze the degree of methylation and to produce images (<http://quma.cdb.riken.jp/>).

### 2.9. Statistical analysis

All experiments were repeated at least three times. Data are presented as the mean  $\pm$  SD. Statistical significance was assessed using Student's *t*-test. Differences were considered statistically significant at *p* < 0.05.

## 3. Results

### 3.1. Identification of pig ADSCs and MSCs

To verify that the cells that we isolated were ADSCs and MSCs, we analyzed the cells for the expression of selected marker genes and stained the cells using Oil Red O staining to identify adiposities [9]. When ADSCs and MSCs reached 80–90% confluence, the cells were digested with trypsin and seeded onto sterile clean slides for 24 h. Then, the cells were subjected to immunohistochemistry using the stem markers desmin and CD44. As shown in Fig. 1, the vast majority of ADSCs were positive for CD44 but not for desmin (Fig. 1A). However, most of the MSCs expressed desmin and CD44

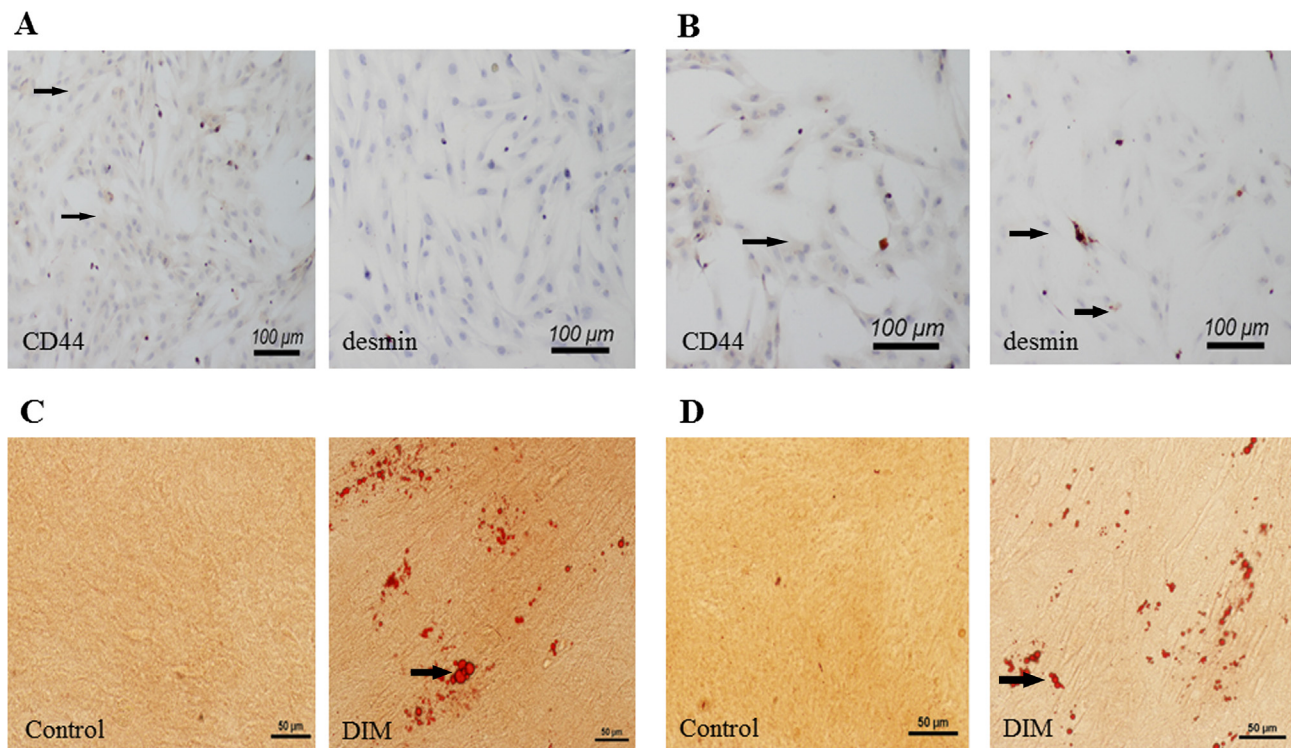


**Fig. 1.** Identification of porcine adipose-derived stem cells (ADSCs) and muscle satellite cells (MSCs). (A) Immunocytochemistry analysis of CD44 and desmin expression in ADSCs. (B) Immunocytochemistry analysis of CD44 and desmin expression in MSCs. (Positive reactions are indicated in brown, arrowheads). (C) ADSCs were treated with DIM and then stained with Oil Red O. (D) MSCs were treated with DIM and then stained with Oil Red O. (For interpretation of the references to colour in this figure legend, the reader is referred to the web version of this article.)



(Fig. 1B). The Oil Red O staining results showed that the cells treated with DIM had a greater accumulation of triglycerides in lipid droplets on the 8th day of differentiation compared with control cells (Fig. 1C and D).

### 3.2. *PPAR $\gamma$* and *MyoD* mRNA levels

qPCR gene expression analysis was performed on ADSCs and MSCs treated with 100 ng/mL MSTN for 0, 24, and 48 h. The results demonstrated that *PPAR $\gamma$*  and *MyoD* mRNA levels significantly ( $p < 0.05$ ) increased by 2.76-fold and 8.33-fold, respectively, at 48 h compared with the 0 h time point in ADSCs; however, significant differences were not noted between 0 and 24 h (Fig. 2A). In MSCs, the expression of *PPAR $\gamma$*  and *MyoD* significantly decreased from 0 to 48 h (Fig. 2B).

### 3.3. *PPAR $\gamma$* and *MyoD* protein expression analysis

According to Western blot analysis, the *PPAR $\gamma$*  and *MyoD* protein levels increased in ADSCs after treatment with MSTN (Fig. 3A); however, *PPAR $\gamma$*  and *MyoD* protein expression levels decreased from 0 to 48 h in MSCs (Fig. 3B), which was generally consistent with the qPCR results.

### 3.4. *PPAR $\gamma$* and *MyoD* promoter CpG island methylation analysis

We used the software MethPrimer to analyze the CpG islands in the *PPAR $\gamma$*  and *MyoD* promoter region. The CpG island of the *PPAR $\gamma$*  promoter was in the –2094 to –1994 region, and the CpG island of the *MyoD* promoter was in the –587 to –427 region. Then, we

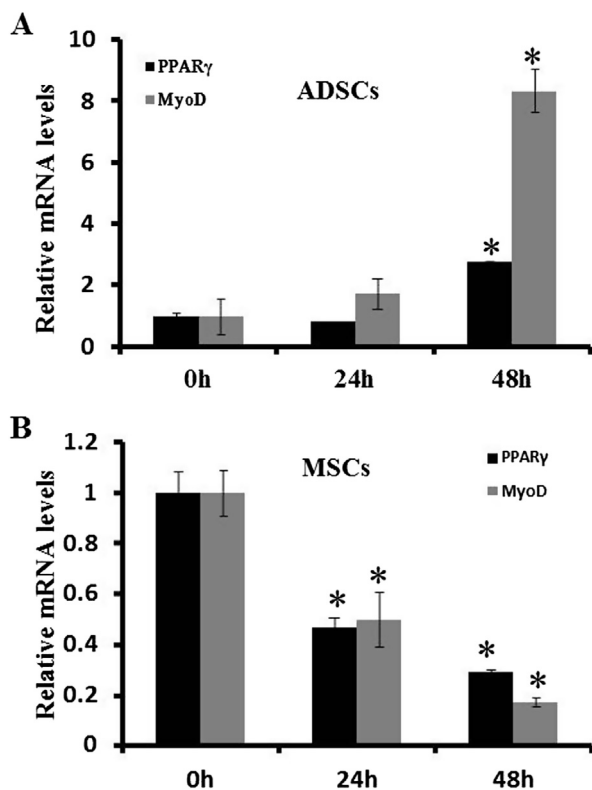


**Fig. 2.** Quantitative real-time PCR analysis of *PPAR $\gamma$*  and *MyoD* gene expression levels in adipose-derived stem cells (ADSCs) and muscle satellite cells (MSCs). Cells were treated with 100 ng/mL MSTN for 0, 24, or 48 h (A) *PPAR $\gamma$*  and *MyoD* gene expression levels in ADSCs. (B) *PPAR $\gamma$*  and *MyoD* gene expression levels in MSCs. (Values are the mean  $\pm$  SD;  $n = 3$ ; \* $p < 0.05$ ).

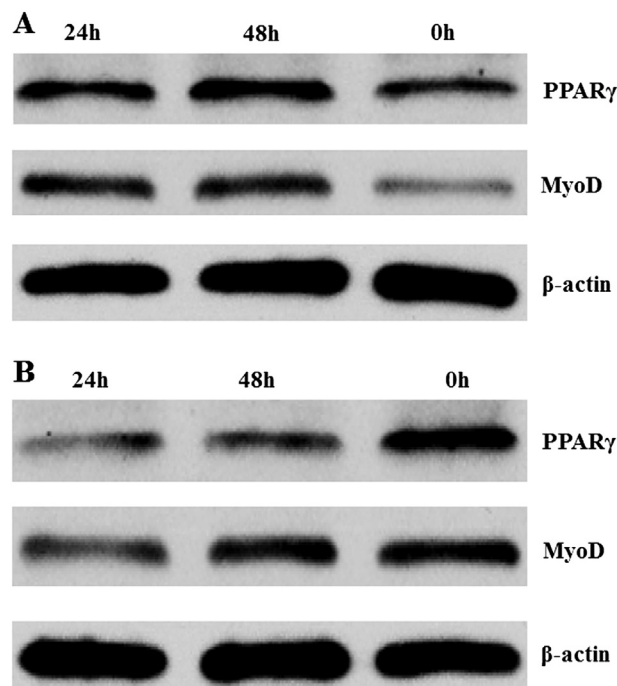


**Fig. 3.** Western blot analysis of *PPAR $\gamma$*  and *MyoD* protein expression levels in adipose-derived stem cells (ADSCs) and muscle satellite cells (MSCs). Cells were treated with 100 ng/mL MSTN for 0, 24, or 48 h (A) *PPAR $\gamma$*  and *MyoD* expression levels in ADSCs. (B) *PPAR $\gamma$*  and *MyoD* expression levels in MSCs.

amplified a 162-bp fragment from –2127 to –1966 of *PPAR $\gamma$*  and a 224-bp fragment from –645 to –422 of *MyoD*.

The methylation of the *PPAR $\gamma$*  promoter CpG islands in ADSCs treated with MSTN increased from 0 to 24 h and then decreased from 24 to 48 h (Fig. 4A), while the methylation of the *MyoD* promoter CpG islands decreased compared with untreated controls (Fig. 4B). The methylation of *PPAR $\gamma$*  (Fig. 4C) and *MyoD* (Fig. 4D) increased when MSCs were treated with MSTN.

## 4. Discussion

Adipose cells differentiate from preadipocytes in a lipogenic environment in fat tissues [13,19]. However, as the environment in muscle tissue differs from that of fat tissue, adipocytes in muscle may differentiate from the stem cells found in muscle, such as ADSCs and MSCs [3,6–8]. Previous work demonstrated that MSTN, a protein secreted from muscle tissue [20–23], inhibits the adipogenic potential of MSCs but not ADSCs; this result indicates that muscle adipocytes may differentiate from ADSCs but not MSCs [9]. In this study, we sought to elucidate how MSTN differentially regulates ADSCs and MSCs adipogenesis.

First, we isolated ADSCs and MSCs according to previously reported methods [16,17]. Then, we examined the expression of desmin and CD44 in ADSCs and MSCs using immunocytochemistry. Our results (Fig. 1A and B) were identical to results reported by Deng et al. [9] and indicated that the cells were two different types of stem cells. Furthermore, the Oil Red O staining results indicated that ADSCs and MSCs have the potential to undergo adipogenesis.

*PPAR $\gamma$*  is a critical transcription factor that primarily triggers the expression of genes responsible for adipogenesis [24] and triglyceride storage in adipose cells [13]. Until now, no factor has been discovered that promotes adipogenesis in the absence of *PPAR $\gamma$*  [25]. In this study, we used qPCR and Western blotting to examine *PPAR $\gamma$*  mRNA and protein levels in ADSCs treated with MSTN before differentiation. The results indicate that *PPAR $\gamma$*  expression was

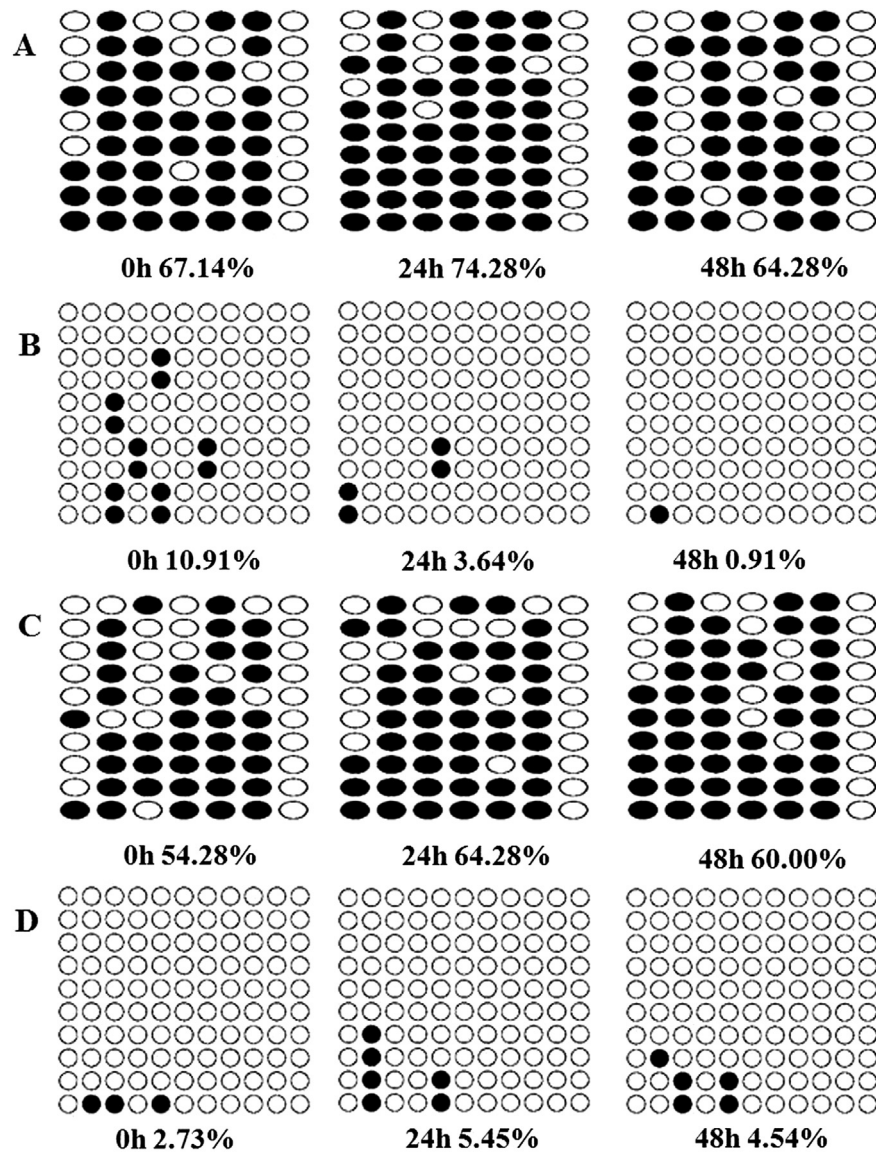


**Fig. 4.** The DNA methylation status of the CpG islands in the *PPAR $\gamma$*  and *MyoD* promoters was quantified using bisulfite sequencing PCR, and a minimum of ten positive clones were randomly picked for sequencing with M13 primers. Sequencing results were visualized using the QUMA software. White circles correspond to unmethylated Cs, and black circles correspond to methylated Cs. Genomic DNA was isolated from adipose-derived stem cells (ADSCs) and muscle satellite cells (MSCs). Cells were treated with 100 ng/mL MSTN for 0, 24, or 48 h (A) *PPAR $\gamma$*  gene methylation status in ADSCs. (B) *MyoD* gene methylation status in ADSCs. (C) *PPAR $\gamma$*  gene methylation status in MSCs. (D) *MyoD* gene methylation status in MSCs.

increased following treatment. Promoter methylation can stably alter gene expression, generally by suppressing target genes [26–28]. As shown in Fig. 4A, we found that the *PPAR $\gamma$*  promoter methylation pattern inversely correlated with its mRNA levels. *PPAR $\gamma$*  expression may indicate that the adipogenic potential was activated by MSTN in ADSCs prior to differentiation.

MSCs reside as quiescent cells underneath the basal lamina that surrounds muscle fibers and play a principal role in postnatal skeletal muscle growth and maintenance [29]. These cells can differentiate into multiple tissue lineages, including adipocytes, osteoblasts, and myoblasts [3,7]. Our previous study indicated that MSCs possess adipogenic potential, but this potential is lost when treated with MSTN [9]. When we treated MSCs with MSTN, *PPAR $\gamma$*  mRNA and protein levels decreased from 0 to 48 h. *PPAR $\gamma$*  promoter methylation exhibited the opposite trend. Inhibiting *PPAR $\gamma$*  expression may represent the loss of adipogenic potential in MSCs. Moreover, differential *PPAR $\gamma$*  expression patterns at the mRNA and

protein levels may indicate that MSTN differentially regulates *PPAR $\gamma$*  to determine the adipogenic potential of ADSCs and MSCs. Based on the methylation results of the *PPAR $\gamma$*  promoter, we hypothesized that MSTN differentially regulates *PPAR $\gamma$*  expression through methylation of the promoter region in ADSCs and MSCs.

In this study, *MyoD* mRNA and protein levels decreased in MSCs after treatment with MSTN, but their levels increased in MSTN-treated ADSCs. These expression results were inversely correlated with the methylation results. *MyoD* is a transcription factor involved in the regulation of muscle development [10]. Hennebry et al. [30] found that MSTN negatively regulates *MyoD* expression in muscle tissue. Furthermore, it also regulates muscle satellite cell proliferation and suppresses the differentiation of myoblasts into myotubes through the down-regulation of *MyoD* [23,31]. Given the *PPAR $\gamma$*  and *MyoD* expression patterns in MSCs, we hypothesized that the inhibition of *MyoD* activity by MSTN may result in MSC proliferation and the loss of differentiation potential, including

adipogenesis and myogenesis. Forced expression of *MyoD* in vitro has been shown to induce myogenic differentiation while inhibiting adipogenic differentiation in mesenchymal stem cells [32]. Because *PPAR $\gamma$*  and *MyoD* were activated by MSTN in ADSCs and adipogenic differentiation was not inhibited in our previous study [9], we thought that MSTN-induced *MyoD* expression would not produce adipogenic inhibition in ADSCs. The actual role of *MyoD* in MSTN-treated ADSCs requires further study.

Rebbapragada et al. [33] found that MSTN could bind the type-II Ser/Thr kinase receptor (ActRIIB) and partner with a type-I receptor, either activin receptor-like kinase 4 (ALK4 or ActRIB) or ALK5 (T $\beta$ RI), to induce Smad2/3 (SMAD family member 2/3) phosphorylation and thus inhibit adipogenesis in C3H10T1/2 cells. In this study, the expression of *PPAR $\gamma$*  and *MyoD* differed in ADSCs and MSCs. We propose that MSTN signaling can be transmitted to the cell nuclei through different mechanisms in these two cell types.

ADSCs and MSCs are two types of stem cells in muscle that exhibit adipogenic potential. When these stem cells are in a lipogenic and MSTN-secreted environment, ADSCs will exhibit adipogenic potential because of MSTN-induced *PPAR $\gamma$*  and *MyoD* expression. However, in MSCs, *PPAR $\gamma$*  and *MyoD* expression were inhibited by MSTN, thus inhibiting adipogenesis. From these results, we hypothesized that the adipogenic regulatory roles of MSTN in ADSCs and MSCs were attributed to the differential regulation of *PPAR $\gamma$*  and *MyoD*. Furthermore, these results could provide greater understanding of the adipocytes in muscle, which mainly arise from ADSCs.

## Conflict of interest

The authors declare no conflict of interest.

## Acknowledgments

This research was supported by the National Natural Science Foundation of China (31201766), the National Science & Technology Pillar Program during the Twelfth Five-year Plan Period (2011BAD28B01), the Science and Technology Planning Project of Hubei Province, China (2011BBB090), the Elite Project of Wuhan Institute of Agricultural Science and Technology (YC201202), and a grant from the National Project for Breeding of Transgenic Pig (2013ZX08006-002).

## Transparency document

Transparency document related to this article can be found online at <http://dx.doi.org/10.1016/j.bbrc.2015.01.120>.

## References

- [1] D.W. P. G.S. Harper, How might marbling begin? *Aust. J. Exp. Agric.* 44 (2004) 653–662.
- [2] S.-H. Lee, E.-W. Park, Y.-M. Cho, S.-K. Kim, J.-H. Lee, J.-T. Jeon, C.-S. Lee, S.-K. Im, S.-J. Oh, J.M. Thompson, D. Yoon, Identification of differentially expressed genes related to intramuscular fat development in the early and late fattening stages of hanwoo steers, *J. Biochem. Mol. Biol.* 40 (2007) 757–764.
- [3] X. Zhou, D. Li, J. Yin, J. Ni, B. Dong, J. Zhang, M. Du, CLA differently regulates adipogenesis in stromal vascular cells from porcine subcutaneous adipose and skeletal muscle, *J. Lipid Res.* 48 (2007) 1701–1709.
- [4] B.H. Goodpaster, S. Krishnaswami, H. Resnick, D.E. Kelley, C. Haggerty, T.B. Harris, A.V. Schwartz, S. Kritchevsky, A.B. Newman, Association between regional adipose tissue distribution and both type 2 diabetes and impaired glucose tolerance in elderly men and women, *Diabetes Care* 26 (2003) 372–379.
- [5] J.B. Albu, A.J. Kovera, L. Allen, M. Wainwright, E. Berk, N. Raja-Khan, I. Janumala, B. Burkey, S. Heshka, D. Gallagher, Independent association of insulin resistance with larger amounts of intermuscular adipose tissue and a greater acute insulin response to glucose in African American than in white nondiabetic women, *Am. J. Clin. Nutr.* 82 (2005) 1210–1217.
- [6] D.W. Pethick, G.S. Harper, V.H. Oddy, Growth, development and nutritional manipulation of marbling in cattle: a review, *Aust. J. Exp. Agric.* 44 (2004) 705–715.
- [7] G. Shefer, M. Wlekinski-Lee, Z. Yablonka-Reuveni, Skeletal muscle satellite cells can spontaneously enter, an alternative mesenchymal pathway, *J. Cell Sci.* 117 (2004) 5393–5404.
- [8] A. Asakura, M. Komaki, M.A. Rudnicki, Muscle satellite cells are multipotential stem cells that exhibit myogenic, osteogenic, and adipogenic differentiation, *Differentiation* 68 (2001) 245–253.
- [9] B. Deng, J.H. Wen, Y. Ding, J. Peng, S.W. Jiang, Different regulation role of myostatin in differentiating pig ADSCs and MSCs into adipocytes, *Cell Biochem. Funct.* 30 (2012) 145–150.
- [10] J.N. Artaza, S. Bhasin, T.R. Magee, S. Reisz-Porszasz, R.Q. Shen, N.P. Groome, M.M. Fareez, N.F. Gonzalez-Cadavid, Myostatin inhibits myogenesis and promotes adipogenesis in C3H 10T1/2 mesenchymal multipotent cells, *Endocrinology* 146 (2005) 3547–3557.
- [11] H.S. Kim, L. Liang, R.G. Dean, D.B. Hausman, D.L. Hartzell, C.A. Baile, Inhibition of preadipocyte differentiation by myostatin treatment in 3T3-L1 cultures, *Biochem. Biophys. Res. Commun.* 281 (2001) 902–906.
- [12] F.M. Gregoire, C.M. Smas, H.S. Sul, Understanding adipocyte differentiation, *Physiol. Rev.* 78 (1998) 783–809.
- [13] E.D. Rosen, C.J. Walkey, P. Puigserver, B.M. Spiegelman, Transcriptional regulation of adipogenesis, *Genes Dev.* 14 (2000) 1293–1307.
- [14] T. Kazama, M. Fujie, T. Endo, K. Kano, Mature adipocyte-derived dedifferentiated fat cells can transdifferentiate into skeletal myocytes in vitro, *Biochem. Biophys. Res. Commun.* 377 (2008) 780–785.
- [15] M. Manceau, J. Gros, K. Savage, V. Thome, A. McPherron, B. Paterson, C. Marcelle, Myostatin promotes the terminal differentiation of embryonic muscle progenitors, *Genes Dev.* 22 (2008) 668–681.
- [16] B.A. Bunnell, M. Flaet, C. Gagliardi, B. Patel, C. Ripoll, Adipose-derived stem cells: isolation, expansion and differentiation, *Methods* 45 (2008) 115–120.
- [17] K. Yamanouchi, A. Ban, S. Shibata, T. Hosoyama, Y. Murakami, M. Nishihara, Both *PPAR* gamma and *C/EBP* alpha are sufficient to induce trans-differentiation of goat fetal myoblasts into adipocytes, *J. Reprod. Dev.* 53 (2007) 563–572.
- [18] K.J. Livak, T.D. Schmittgen, Analysis of relative gene expression data using real-time quantitative PCR and the 2- $\Delta\Delta$ CT method, *Methods (Orlando)* 25 (2001) 402–408.
- [19] N.H. Haunerland, F. Spener, Fatty acid-binding proteins - insights from genetic manipulations, *Prog. Lipid Res.* 43 (2004) 328–349.
- [20] S. Hirai, H. Matsumoto, N. Hino, H. Kawachi, T. Matsui, H. Yano, Myostatin inhibits differentiation of bovine preadipocyte, *Domest. Anim. Endocrinol.* 32 (2007) 1–14.
- [21] T.Q. Guo, W. Jou, T. Chanturiya, J. Portas, O. Gavrilova, A.C. McPherron, Myostatin inhibition in muscle, but not adipose tissue, decreases fat mass and improves insulin sensitivity, *Plos One* 4 (2009).
- [22] M.W. Hamrick, X. Shi, W. Zhang, C. Pennington, H. Thakore, M. Haque, B. Kang, C.M. Isles, S. Fulzele, K.H. Wenger, Loss of myostatin (*GDF8*) function increases osteogenic differentiation of bone marrow-derived mesenchymal stem cells but the osteogenic effect is ablated with unloading, *Bone* 40 (2007) 1544–1553.
- [23] B. Langley, M. Thomas, A. Bishop, M. Sharma, S. Gilmour, R. Kambadur, Myostatin inhibits myoblast differentiation by down-regulating *MyoD* expression, *J. Biol. Chem.* 277 (2002) 49831–49840.
- [24] D. Holst, S. Luquet, V. Nogueira, K. Kristiansen, X. Leverve, P.A. Grimaldi, Nutritional regulation and role of peroxisome proliferator-activated receptor delta in fatty acid catabolism in skeletal muscle, *Biochim. Biophys. Acta Mol. Cell Biol. Lipids* 1633 (2003) 43–50.
- [25] P. Tontonoz, B.M. Spiegelman, Fat and Beyond: The Diverse Biology of PPAR Gamma, *Annual Review of Biochemistry, Annual Reviews, Palo Alto*, 2008, pp. 289–312.
- [26] M. Volkmar, S. Dedeurwaerder, D.A. Cunha, M.N. Ndlovu, M. Defrance, R. Deplus, E. Calonne, U. Volkmar, M. Igoillo-Esteve, N. Naamane, DNA methylation profiling identifies epigenetic dysregulation in pancreatic islets from type 2 diabetic patients, *EMBO J.* 31 (2012) 1405–1426.
- [27] R. Barres, J.R. Zierath, DNA methylation in metabolic disorders, *Am. J. Clin. Nutr.* 93 (2011) 897S–900S.
- [28] A. Bird, Perceptions of epigenetics, *Nature* 447 (2007) 396–398.
- [29] A. Sacco, R. Doyonnas, P. Kraft, S. Vitorovic, H.M. Blau, Self-renewal and expansion of single transplanted muscle stem cells, *Nature* 456 (2008) 502–506.
- [30] A. Hennebery, C. Berry, V. Siriatt, P. O'Callaghan, L. Chau, T. Watson, M. Sharma, R. Kambadur, Myostatin regulates fiber-type composition of skeletal muscle by regulating *MEF2* and *MyoD* gene expression, *Am. J. Physiol. Cell Physiol.* 296 (2009) C525–C534.
- [31] F. Gao, T. Kishida, A. Ejima, S. Gojo, O. Mazda, Myostatin acts as an autocrine/paracrine negative regulator in myoblast differentiation from human induced pluripotent stem cells, *Biochem. Biophys. Res. Commun.* 431 (2013) 309–314.
- [32] S. Goudenege, D.F. Pisani, B. Wdziekonski, J.P. Di Santo, C. Bagnis, C. Dani, C.A. Dechesne, Enhancement of myogenic and muscle repair capacities of human adipose-derived stem cells with forced expression of *MyoD*, *Mol. Ther.* 17 (2009) 1064–1072.
- [33] A. Rebbapragada, H. Benchabane, J.L. Wrana, A.J. Celeste, L. Attisano, Myostatin signals through a transforming growth factor beta-like signaling pathway to block adipogenesis, *Mol. Cell Biol.* 23 (2003) 7230–7242.